International Journal of Computational and Experimental Science and ENgineering
(IJCESEN)

Vol. 11-No.2 (2025) pp. 2939-2946
http://www.ijcesen.com

ISSN: 2149-9144

Research Article

A Novel Power-Optimized Optical Modem for Reliable, Long-Distance Communication Using MIMO-GFDM in Underwater Communication and Beyond 5G Wireless Systems

V.Tejovathi[1]*, S.Swarnalatha[2]

[1]Research Scholar, Department of ECE, SVUCE, SV University, Tirupati, A.P, India
* **Corresponding Author Email:** venatitejovathi@gmail.com - **ORCID:** 0009-0009-7098-3069

[2] Professor, Department of ECE, SVUCE, SV University, Tirupati, A.P, India
Email: swarnasvu09@gmail.com - **ORCID:** 0000-0001-6002-1389

Article Info:

DOI: 10.22399/ijcesen.1820
Received : 05 March 2025
Accepted : 17 April 2025

Keywords

MIMO-GFDM
Long-Distance Communication
5G Wireless Systems

Abstract:

MIMO-GFDM is proposed for Underwater Optical Wireless Communication (UWOC) to address challenges like multipath fading, Doppler effects, and bandwidth constraints. Unlike traditional techniques such as OFDM, FBMC, and SC-FDMA, MIMO-GFDM offers reduced OOB emissions, lower ISI, and improved spectral efficiency. By combining MIMO with GFDM, the system enhances SNR, boosts data rates, and minimizes interference. Pulse shaping filters further optimize PAPR, improving overall efficiency. Simulation results show MIMO-GFDM outperforms conventional methods in data rate, BER, and spectral efficiency, making it a strong candidate for next-generation UWOC systems.

1. Introduction

Underwater wireless communication (UWC) is crucial for various applications such as ocean exploration, environmental monitoring, defense, and disaster prevention [1]. However, the underwater environment poses significant challenges, including high path loss, limited bandwidth, multipath fading, and Doppler effects, which degrade the performance of traditional wireless communication systems [2].
Three primary transmission methods have been explored for UWC. Acoustic waves are the most widely used due to their long transmission range, but they suffer from low data rates, high latency, and susceptibility to multipath fading [3]. Optical wireless communication offers high data rates but is affected by water turbidity, scattering, and absorption, limiting its range and reliability [4]. RF signals experience rapid attenuation in water, restricting their range to only a few meters [5].
OFDM has been widely adopted for UWC due to its robustness against multipath fading and efficient spectral utilization [6]. However, it suffers from several drawbacks, such as high out-of-band (OOB) emissions, inter-symbol interference (ISI), and inter-carrier interference (ICI) in dispersive underwater channels [7]. Moreover, the need for a cyclic prefix (CP) reduces spectral efficiency [8].
MIMO-OFDM has been explored as a way to enhance spectral efficiency and increase data rates by leveraging spatial diversity [9]. However, MIMO-OFDM is highly sensitive to synchronization errors and Doppler shifts, which significantly affect its performance in underwater environments [10].
Several alternative multicarrier techniques have been investigated to overcome the limitations of OFDM in UWC. FBMC improves spectral efficiency but complicates MIMO implementation due to the lack of a cyclic prefix [11]. UFMC reduces OOB emissions but increases computational complexity [12]. OTFS exhibits resilience to underwater Doppler variations but requires advanced receiver processing, increasing computational burden [13]. SC-FDMA reduces peak-to-average power ratio (PAPR) but demands complex equalization at the receiver [14].
To improve spectral efficiency further, advanced multiple access schemes such as SCMA and

NOMA have been proposed. SCMA enhances data transmission efficiency but increases receiver complexity due to advanced decoding requirements [15]. NOMA enables multiple users to share time-frequency resources via power-domain multiplexing. However, it faces computational and power allocation challenges in underwater environments [16]. Additionally, research on hybrid optical-acoustic MIMO-OFDM-based modems has been conducted to enhance reliability and high-speed underwater communication [24-25]. These hybrid modems demonstrate significant improvements in data rates while addressing the limitations of individual communication techniques [26]. Despite its advantages, MIMO-GFDM still presents some challenges. Its non-orthogonal nature makes synchronization more complex compared to OFDM-based systems. Advanced receiver algorithms are required for efficient equalization and interference cancellation, adding to computational complexity. Efficient FPGA-based implementations are necessary to ensure real-time processing for underwater communication applications [27].

GFDM has emerged as a promising alternative to traditional multicarrier modulation techniques. Unlike OFDM, GFDM employs non-orthogonal subcarriers with a flexible block-based transmission structure, which enhances spectral efficiency and reduces ISI and OOB emissions [17]. GFDM's time-frequency block structure makes it more robust against underwater channel impairments [18]. It applies pulse shaping with a prototype filter to minimize OOB emissions and PAPR, making it highly suitable for dynamic spectrum allocation in underwater communication without severe interference to incumbent services [19-20]. The integration of MIMO with GFDM has been proposed to leverage spatial diversity and improve system performance. MIMO-GFDM enhances the signal-to-noise ratio (SNR), increases data throughput, and mitigates ICI and ISI, making it a strong candidate for next-generation high-performance UWC systems [21].

Simulation results have demonstrated that MIMO-GFDM outperforms MIMO-OFDM, FBMC, and SC-FDMA in terms of data rate, BER, and spectral efficiency under various underwater conditions [22]. Several studies have analyzed the impact of pulse-shaping filters on the PAPR performance of underwater GFDM systems, confirming its advantages in mitigating nonlinear distortions and improving energy efficiency [23].

Future research should focus on optimizing MIMO-GFDM receiver architectures, improving synchronization techniques, and exploring hybrid communication schemes that integrate GFDM with optical and acoustic systems for enhanced performance. MIMO-GFDM has emerged as a strong alternative to traditional multicarrier modulation techniques for underwater wireless communication. By leveraging its flexible block-based structure, reduced ISI, and improved spectral efficiency, MIMO-GFDM provides a viable solution for overcoming the challenges of UWC. While challenges remain in synchronization and computational complexity, ongoing research suggests that MIMO-GFDM will play a key role in next-generation high-performance UWC systems.

2. Proposed method:

In this section, first GFDM system model is described from the reference [22] and then MIMO-GFDM System model is described. GFDM uses circularly-filtered and multicarrier modulation communication scheme.

2.1 GFDM System Model

Figure 1 shows the block diagram of GFDM in underwater communication system. In the first step, the source data vector $\vec{b}$ is encoded as $\overrightarrow{b_c}$, followed by mapper and GFDM modulator, which modulates mapped data $\vec{d}$. The detailed structure of the modulator is shown in Figure 2. The GFDM modulator plays a similar role as IFFT in OFDM. Vector $\vec{d}$ is the data block with dimension $N \times 1$, which is composed of K subcarriers and M subsymbols and N satisfies the equation $N = K \times M$. After adding CP to the modulated data $\vec{x}$, the data $\vec{x}$ is transmitted through the underwater channel. At the receiving terminal, the channel estimation and equalization are performed after synchronization and CP removal. Finally, the estimated sending data $\vec{\vec{b}}$ is obtained after demapping and decoding.

GFDM uses a circularly-filtered multicarrier non-orthogonal modulation scheme. A GFDM consists of K- subcarriers and M- sub symbols. The transmit signal $x[n]$ is given by:

$$x[n] = \sum_{k=0}^{K-1} \sum_{m=0}^{M-1} d_{k,m}\, g_{k,m}\,[n] \qquad (1)$$

Where $n = 0,1, \dots, N-1$

Where $d_{k,m}$ denotes data sub symbol, and $g_{k,m}[n]$ is the circularly shifted transmit filter:

$$g_{k,m}[n] = g[(n - mK)_{mod\ N}] exp\left({}^{-j2\pi nk}/_{K}\right) \qquad (2)$$

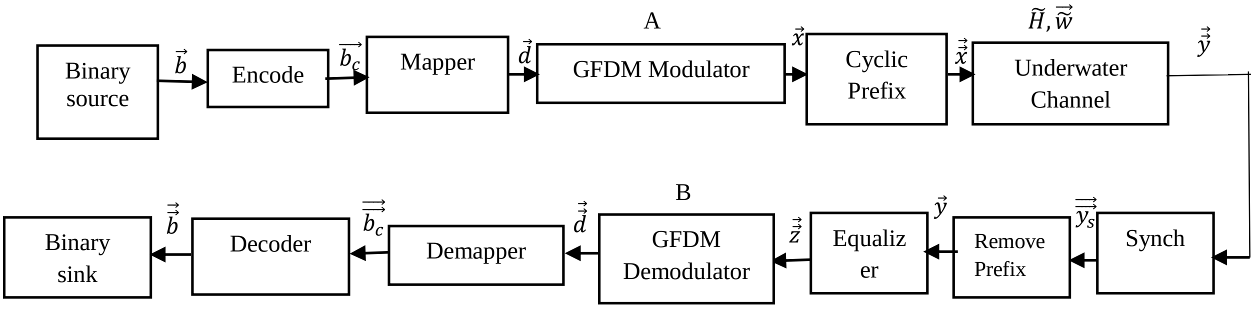

Figure 1. *Block Diagram of the GFDM*

In a vector form $g_{k,m} = [g_{k.m}[0], g_{k.m}[1] \dots g_{k.m}[N-1]]^T$ allows us to formulate (1) as:

$$\vec{x} = A\vec{d} \qquad (3)$$

where d is a data column vector, A is a transmitter matrix represents as a

$$A = \left(g_{0,0} \cdots g_{K-1,0}\ g_{0,1} \cdots g_{K-1,1} \cdots g_{K-1,M-1}\right) \qquad (4)$$

Finally, adding a cyclic prefix (CP) in order to avoid inter-symbol interference (ISI). At the receiver side, the received signal after CP removal can be expressed as:

$$y = Cx + w = CAd + w \qquad (5)$$

Where C is the circular convolution matrix and w is AWGN. After zero-forcing (ZF) equalization,

$$z = C^{-1}CAd + C^{-1}w = Ad + \overline{w} \qquad (6)$$

Finally, the demodulation of the signal can be expressed as:

$$\vec{d} = Bz \qquad (7)$$

where B can be a matched filter $B_{MF} = A^H$, ZF receiver $B_{ZF} = A^{-1}$, and minimum mean square error (MMSE) receiver $B_{MMSE} = (R_W + A^H A)^{-1} A^H$. For jointly equalize and detect without a separate ZF block.

Figure 2 illustrates the GFDM modulator, where $d_{k,m}$, denotes the data transmitted on the K^{th} subcarrier and, in the M^{th} subsymbol of the block, This data is shaped by the corresponding pulse shaping filter $g_{k,m}$.

The comparison of time and frequency division among OFDM, SC-FDE, and GFDM is presented in Figure 3. From this comparison, it can be inferred that GFDM generalizes both OFDM and SC-FDE. Specifically, when $M = 1$, $K = N$, GFDM simplifies to OFDM. Conversely, setting $M = N$ and $K = 1$ SC-FDE is obtained As a result, the Peak-to-Average Power Ratio (PAPR) of GFDM is expected to fall between the PAPR values of OFDM and SC-FDE.

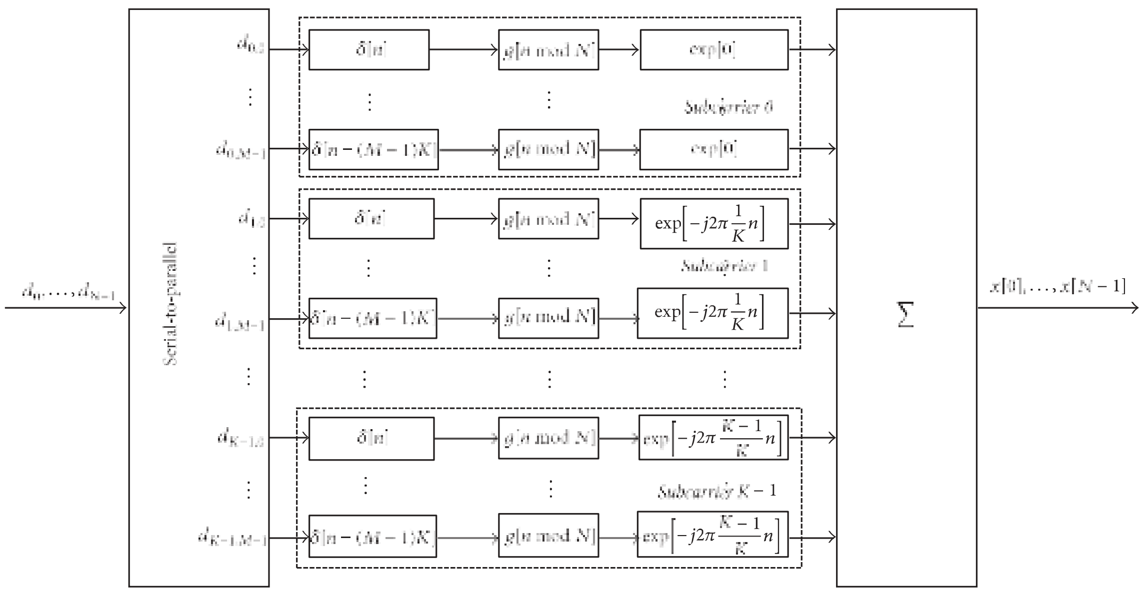

Figure 2. *Modulator of the GFDM*

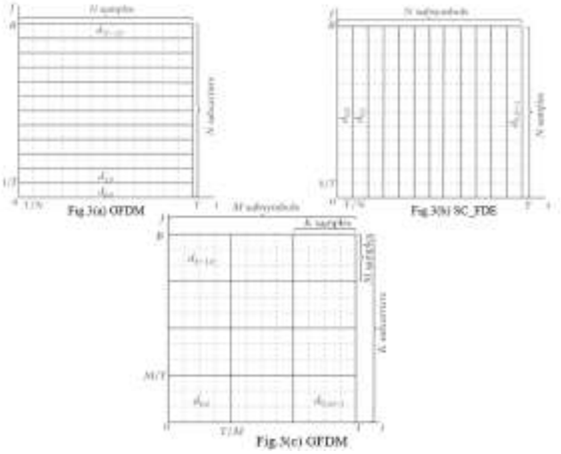

Figure 3. *time and frequency division of different modulation schemes*

2.2 PAPR of GFDM

The Peak-to-Average Power measures the ratio of a peak power of a signal to its average power. Mathematically, PAPR is defined as:

$$PAPR = \frac{Maximum\ Instantaneous\ power}{Average\ power} \qquad (8)$$

Or in decibels (dB):

$$PAPR(dB) = 10\,log_{10}(\frac{max(|x_n|^2)}{E[|x_n|^2]}) \qquad (9)$$

A discrete GFDM signal is given in

$$\vec{x}(n) = \sum_{k=0}^{K-1}\sum_{m=0}^{M-1} g_{k,m}[n]d_{k,m}e^{-j(2\pi nk/K)} \qquad (10)$$

where $g_{k,m}[n]$ is the filtered data and $d_{k,m}$ is the transmitted symbol. GFDM's overlapping structure can result in peak power up to M- times the average. Therefore, the PAPR of GFDM signal is expressed as

$$PAPR(dB) = 10\,log_{10}\frac{max_{0\le n\le N-1}(|x_n|^2)}{E[|x_n|^2]} \qquad (11)$$

where $E[\cdot]$ is mathematical expectation and x_n represents the discrete GFDM signal in time domain.

2.3 MIMO-GFDM System Model

The integration of MIMO with GFDM enhances spectral efficiency and SNR. For an $N_t \times N_r$ MIMO-OFDM channel, the received vector y_k of the K^{th} subcarrier can be expressed as:

$$y_k = H_k x_k + w_k \qquad (12)$$

where N is the number of subcarriers, w_k is the channel noise vector, H_k is the $N_t \times N_r$ frequency response channel matrix, and x_k is the transmit data vector at the K^{th} subcarrier frequency. Since each GFDM block has K subcarriers, the same model can be used for MIMO-GFDM application. In the MIMO-GFDM receiver, a K-point FFT is required for each received signal vector after CP removal.

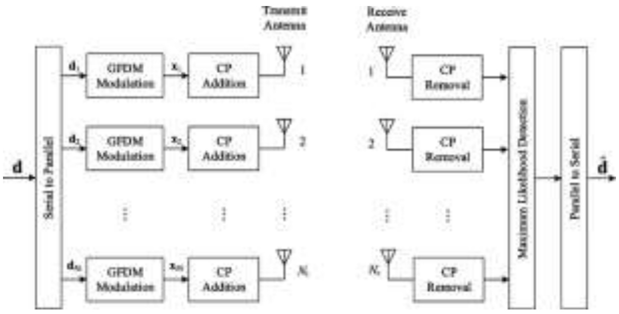

Figure 4. *GFDM with MIMO system model*

The optimal GFDM receiver must manage ICI, ISI, IAI, and IAS in MIMO systems, increasing complexity. A low-complexity MIMO-GFDM design is crucial for IoT devices with power and space constraints in future 5G networks.

3. Design of A Proposed Optical Modem Using Mimo-Gfdm

This work proposes a modem design for underwater wireless communication using a MIMO-GFDM system, with performance evaluated through simulation. Figure 5 illustrates the proposed design, featuring a MIMO system with GFDM and Space-Time Coding. Below is a brief block description.

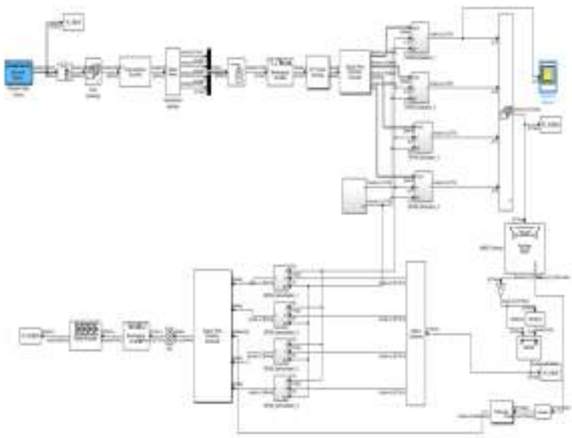

Figure 5. *Proposed MIMO-GFDM based modem design for underwater communication.*

3.1 Transmitter Section

1. **Bernoulli Binary Random Data Source:** It generates random binary sequences for testing digital modulation, error correction, and signal processing.
2. **Input Packing:** Converts incoming bits into symbols based on modulation requirements, ensuring data structure compatibility for encoding and modulation.
3. **Convolutional Encoder:** Adds redundancy for error correction using shift registers and XOR. Supports coding rates like 1/2, 2/3, or 3/4 to correct transmission errors. Common in Wi-Fi, LTE, and 5G.
4. **Subchannel Selector:** Divides encoded data into subchannels for efficient spectrum use, enabling parallel transmission in GFDM and other multicarrier systems.
5. **Rectangular 16-QAM Modulator:** Maps bit groups to complex symbols (e.g., 4 bits to 16-QAM) for higher spectral efficiency. Used in 4G, 5G, and Wi-Fi for fast data transmission.
6. **IFFT Input Packing:** Prepares data for IFFT by arranging subchannel data in frequency bins, essential for GFDM, OFDM, and similar techniques.

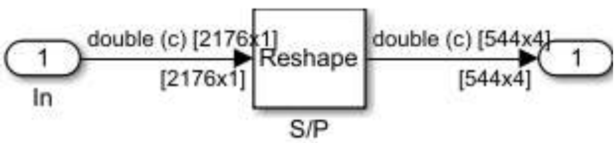

Figure 6. *Internal structure of input packing*

Space-Time Encoder: Improves MIMO reliability using techniques like STBC, distributing symbols across antennas and time slots for diversity gain. Common in Wi-Fi, LTE, and 5G.

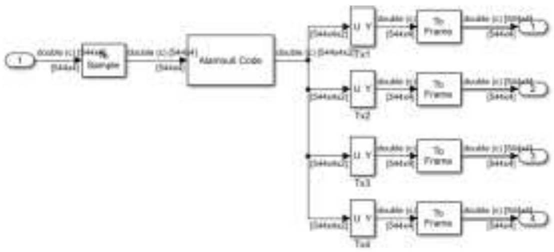

Figure 7. *Structure of Space-Time Block Coding*

7. **GFDM Modulators (1-4):** Applies GFDM modulation with non-orthogonal subcarriers, reducing OOB emissions. Enables flexible spectrum use, low latency, and high efficiency, ideal for IoT, 5G, and cognitive radio.

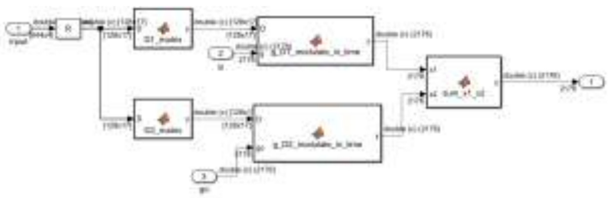

Figure 8. *Structure of GFDM Modulator*

3.2 Channel section

1. **MIMO Channel (Rayleigh Fading):** Simulates MIMO channel with Rayleigh fading, modeling multipath environments without LoS. Suitable for urban/indoor settings, with independent fading per path defined by a probability density function (PDF):

$$p(r) = \frac{r}{\sigma^2} e^{-r^2/2\sigma^2} \qquad (13)$$

where r is the signal amplitude and σ^2 is the average power.
Simulates real-world fading in Wi-Fi, LTE, and 5G to aid MIMO design with techniques like STBC and beamforming.

2. **AWGN (Additive White Gaussian Noise):** Adds Gaussian noise to simulate interference, with

$$N(t) = N\,(0, \sigma^2) \qquad (14)$$

where σ^2 represents the noise power. Ensures flat spectral density, aiding BER vs. SNR evaluation in communication systems.

3. **Path Gain Calculation:** Models channel effects on signal amplitude and phase, accounting for fading, path loss, and multipath. Uses Rayleigh distribution for path gain and may include Doppler effects. Supports equalization, power control, and beamforming.

3.3 Receiver Section

1. **GFDM Demodulators (1-4)**: Demodulates the received Generalized Frequency Division Multiplexing (GFDM) signals. Performs inverse GFDM processing to extract the transmitted symbols. Uses matched filtering and equalization to mitigate inter-symbol interference (ISI) and inter-carrier interference (ICI).
Recovers subcarrier data that was modulated during transmission. Used in 5G, cognitive radio, and IoT applications where spectral efficiency is critical. Helps reduce out-of-band emissions and enhances flexible spectrum use.

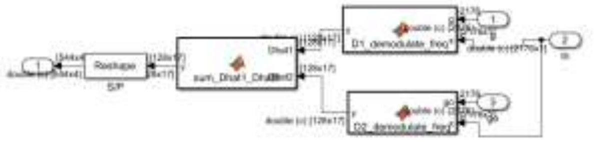

Figure 8. *Structure of GFDM Demodulator*

2. **Space-Time Diversity Combiner:** Combines signals from multiple antennas using methods like MRC, EGC, or Alamouti decoding to improve detection, enhance signal quality, and reduce fading in MIMO systems.
3. **Rectangular 16-QAM Demodulator**: Converts 16-QAM symbols to binary data using decision boundaries for accurate classification. Ensures high spectral efficiency in systems like LTE, Wi-Fi, and DVB.
4. **Viterbi Decoder**: Decodes convolutional codes using dynamic programming and a Trellis diagram. Supports hard or soft decision decoding for error correction in LTE, 5G, Wi-Fi, and satellite communications.
5. **Output Signal Analysis (Rx Output & Analyzer Scope):** Evaluates signal performance using BER, SNR, and constellation diagrams. Visualizes distortions, noise, and errors to optimize modulation and error correction in communication systems.

4. Simulation and Results

The BER vs. Eb/No plot shows system performance as SNR increases. At low Eb/No (0–30 dB), BER remains high (~0.5) due to noise. Beyond 30 dB, BER decreases, indicating improved signal quality. The initial plateau suggests channel impairments or non-ideal performance at low SNR.

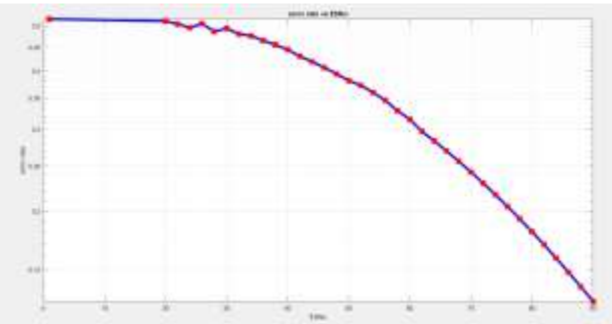

Figure 9. *The Bit Error Rate (BER) vs. Eb/No plot for optical signal*

The PSD plot shows a band-limited signal (0–50 MHz) with power levels around -70 to -80 dB/Hz. The flat spectrum with periodic variations indicates GFDM modulation, ensuring efficient bandwidth use and minimal OOB emissions.

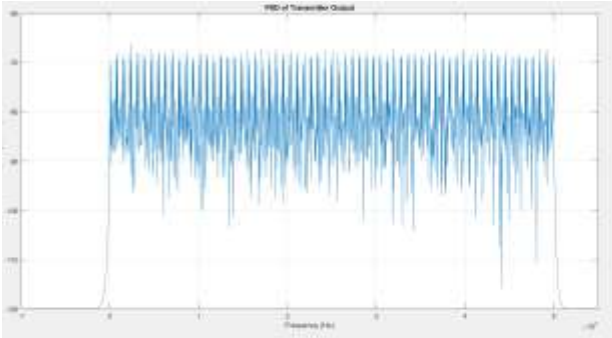

Figure 10. *The Power Spectral Density (PSD) plot of the transmitter output*

The graph shows a binary input signal with bit values (0 and 1) plotted by position, resembling a pseudorandom bit sequence (PRBS) used in digital communication for testing and transmission.

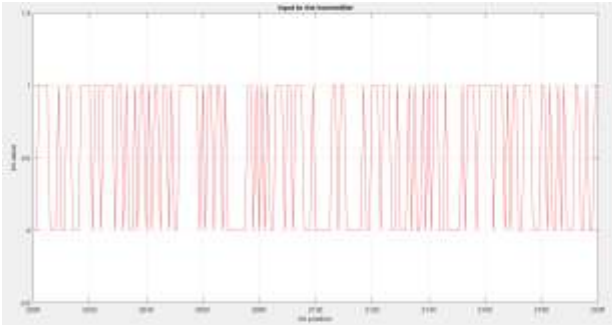

Figure 11. *The binary input signal to the transmitter*

The graph shows the receiver's binary output signal, closely matching the transmitter's input, indicating successful data reception with minimal errors, though slight distortions may suggest noise or channel effects.

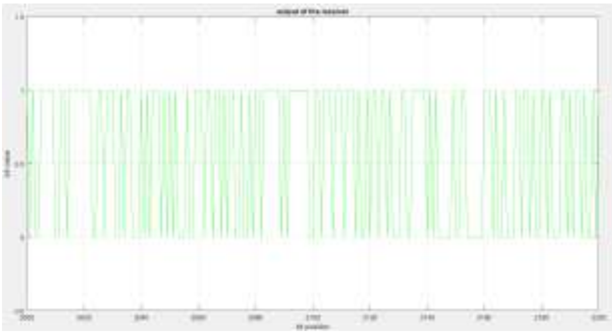

Figure 12. *The binary output signal of the receiver*

The obtained bandwidth is approximately 120 kHz, spanning from -50 kHz to +70 kHz, with power concentrated around the center frequency in a bell-shaped distribution. The signal gradually attenuates towards the edges, indicating primary spectrum utilization.

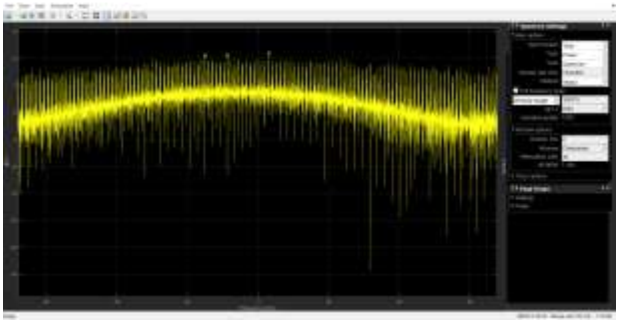

Figure 13. *System bandwidth usage for optical signals in underwater communication*

5. Conclusion:

A novel MIMO-GFDM system utilizing multi carrier modulation is proposed and analyzed using MATLAB Simulink R2020a for optical wireless communication. The system effectively mitigates IAI and IAS, reducing detection complexity while maintaining low PAPR, high spectral efficiency, and low OOB emissions. Despite a slight BER performance loss due to non-orthogonal subcarriers, MIMO-GFDM offers flexibility, time-frequency error tolerance, and reduced system complexity, making it a promising candidate for future 5G optical wireless networks. Additionally, the influence of pulse shaping filters on PAPR is evaluated, confirming GFDM's advantage in bandwidth-limited optical systems. Further research will explore on FBMC-based algorithm applications for high-speed optical communication.

Author Statements:

- **Ethical approval:** The conducted research is not related to either human or animal use.
- **Conflict of interest:** The authors declare that they have no known competing financial interests or personal relationships that could have appeared to influence the work reported in this paper
- **Acknowledgement:** The authors declare that they have nobody or no-company to acknowledge.
- **Author contributions:** The authors declare that they have equal right on this paper.
- **Funding information:** The authors declare that there is no funding to be acknowledged.
- **Data availability statement:** The data that support the findings of this study are available on request from the corresponding author. The data are not publicly available due to privacy or ethical restrictions.

References

[1] Heidemann J., Stojanovic M., & Zorzi M. (2012). Underwater sensor networks: applications, advances, and challenges. *Philosophical Transactions of the Royal Society A*. 370(1958);158-175. https://doi.org/10.1098/rsta.2011.0214

[2] Chitre M., Shahabudeen S., & Stojanovic M. (2008). Underwater acoustic communications and networking: Recent advances and future challenges. *Marine Technology Society Journal*. 42(1);103-116. https://doi.org/10.4031/002533208786861263

[3] Yan H., Zhou S., & Shi Z. (2013). Optimal design of OFDM-based underwater acoustic communication systems. *IEEE Journal of Oceanic Engineering*. 38(4);658-672.

[4] Berkhovskikh L. & Lysanov Y. (2002). Optimal design of OFDM-based underwater acoustic communication systems. *Springer*.

[5] Che X., Wells I., Dickers G., Kear P., & Gong X. (2010). Re-evaluation of RF electromagnetic communication in underwater sensor networks. *IEEE Communications Magazine*. 48(12);143-151. https://doi.org/10.1109/mcom.2010.5673085

[6] Li B., Zhou S., Stojanovic M., Freitag L., & Willett P. (2008). Multicarrier communication over underwater acoustic channels with nonuniform Doppler shifts. *IEEE Journal of Oceanic Engineering*. 33(2);198-209. https://doi.org/10.1109/joe.2008.920471

[7] Stojanovic M. (2008). Underwater acoustic communications: Design considerations on the physical layer. *Wireless on Demand Network Systems and Services*. 2008;1-10. https://doi.org/10.1109/wons.2008.4459349

[8] Kilfoyle D. B. & Baggeroer A. B. (2000). The state of the art in underwater acoustic telemetry. *IEEE Journal of Oceanic Engineering*. 25(1);4-27. https://doi.org/10.1109/48.820733

[9] Goldsmith A. (2005). Wireless Communications. *Cambridge University Press*.

[10] Farhang-Boroujeny B. (2011). OFDM versus filter bank multicarrier. *IEEE Signal Processing Magazine*. 28(3);92-112. https://doi.org/10.1109/msp.2011.940267

[11] Fettweis G., Krondorf M., & Bittner S. (2009). GFDM—Generalized frequency division multiplexing. *Proceedings of the IEEE 69th Vehicular Technology Conference (VTC). Barcelona, Spain*. 1-4. https://doi.org/10.1109/vetecs.2009.5073571

[12] Datta T., Michailow N., Lentmaier M., & Fettweis G. (2013). GFDM interference cancellation for flexible cognitive radio PHY design. *Proceedings of the IEEE 77th Vehicular Technology Conference (VTC). Dresden, Germany*. 1-5. https://doi.org/10.1109/vtcfall.2012.6399031

[13] Hadani R., Rakib S., Tsatsanis M., & Monk A. (2017). Orthogonal time frequency space modulation. *Proceedings of the IEEE Wireless Communications and Networking Conference (WCNC). San Francisco, CA, USA*. 1-6. https://doi.org/10.1109/WCNC.2017.7925924

[14] Tse D. & Viswanath P. (2005). Fundamentals of Wireless Communication. *Cambridge University Press*.

[15] Hanzo L., Akhtman Y., Wang L., & Jiang M. (2011). MIMO-OFDM for LTE, WiFi, and WiMAX: Coherent versus Non-Coherent and Cooperative Turbo-Transceivers. *Wiley*.

[16] Nikopour H. & Baligh H. (2013). Sparse code multiple access. In *Proceedings of the IEEE 24th Annual International Symposium on Personal, Indoor, and Mobile Radio Communications (PIMRC). London, UK*. 332-336. https://doi.org/10.1109/PIMRC.2013.6666156

[17] Dai L., Wang B., Yuan Y., Han S., I. C., & Wang Z. (2015). Non-orthogonal multiple access for 5G: Solutions, challenges, opportunities, and future research trends. *IEEE Communications Magazine*. 53(9);74-81. https://doi.org/10.1109/mcom.2015.7263349

[18] Michailow N., Matthé M., Gaspar I., Navarro A., Mendes L., Festag A., & Fettweis G. (2014). Generalized frequency division multiplexing for 5th generation cellular networks. *IEEE Transactions on Communications*. 62(9);3045-3061. https://doi.org/10.1109/tcomm.2014.2345566

[19] Matthé M., Mendes L., & Fettweis G. (2014). GFDM in a Gabor transform setting. *IEEE Communications Letters*. 18(8);1379-1382. https://doi.org/10.1109/LCOMM.2014.2332155

[20] Gaspar I., Matthé M., Mendes L., & Fettweis G. (2015). GFDM transceiver using precoding and successive interference cancellation. In *Proceedings of the IEEE 81st Vehicular Technology Conference (VTC). Glasgow, UK*. 1-5. https://arxiv.org/pdf/1506.03350

[21] Wymeersch H., Liang J., Win M. Z., & Dusl S. (2017). 5G mmWave positioning for vehicular networks. *IEEE Wireless Communications*. 24(6);80-86. https://doi.org/10.1109/mwc.2017.1600374

[22] Wu J., Ma X., Qi X., Babar Z., & Zheng W. (2017). Influence of Pulse Shaping Filters on PAPR Performance of Underwater 5G Communication System Technique: GFDM. *Wireless Communications and Mobile Computing*. 4361589;7 pages. https://doi.org/10.1155/2017/4361589

[23] Ch P. & Sreenivasulu G. (2023). A Hybrid Optical-Acoustic Modem Based on MIMO-OFDM for Reliable Data Transmission in Green Underwater Wireless Communication. *Journal of VLSI Circuits and Systems*. 6(1);36-42. https://doi.org/10.31838/jvcs/06.01.06

[24] Ch P. & Sreenivasulu G. (2021). A High-Speed Underwater Wireless Communication Through a Novel Hybrid Opto-Acoustic Modem Using MIMO-OFDM. *Instrumentation Mesure Metrologies*. 20(5);279-287. https://doi.org/10.18280/i2m.200505

[25] Ch P. & Sreenivasulu G. (2023). A Highly Compatible Optical/Acoustic Modem Based on MIMO-OFDM for Underwater Wireless Communication Using FPGA. *International Journal of Electrical and Electronics Research*. 11(4);993-1000. https://doi.org/10.37391/ijeer.110417

[26] Ch P. & Sreenivasulu G. (2023). Performance of a MIMO-OFDM-Based Opto-Acoustic Modem for High Data Rate Underwater Wireless Communication (UWC) System. *Advances in Signal Processing, Embedded Systems and IoT*. 992;Link. https://doi.org/10.1007/978-981-19-8865-3_5

[27] Ch P. & Sreenivasulu G. (2020). A Review on Underwater Acoustic/Optical Modems: Design Issues, Recent Developments, and Challenges in Underwater Communication. *i-manager's Journal on Communication Engineering and Systems*. 9(2);21-40. https://doi.org/10.26634/jcs.9.2.18042